Domain Walls and Their Experimental Signatures in $s + is$ Superconductors

Julien Garaud[1,2,*] and Egor Babaev[1,2]
[1]Department of Physics, University of Massachusetts Amherst, Massachusetts 01003, USA
[2]Department of Theoretical Physics, Royal Institute of Technology, Stockholm, SE-10691, Sweden

(Received 15 August 2013; published 8 January 2014)

Arguments were recently advanced that hole-doped $Ba_{1-x}K_xFe_2As_2$ exhibits the $s + is$ state at certain doping. Spontaneous breaking of time-reversal symmetry in the $s + is$ state dictates that it possess domain wall excitations. Here, we discuss what are the experimentally detectable signatures of domain walls in the $s + is$ state. We find that in this state the domain walls can have a dipolelike magnetic signature (in contrast to the uniform magnetic signature of domain walls $p + ip$ superconductors). We propose experiments where quench-induced domain walls can be stabilized by geometric barriers and observed via their magnetic signature or their influence on the magnetization process, thereby providing an experimental tool to confirm the $s + is$ state.

DOI: 10.1103/PhysRevLett.112.017003 PACS numbers: 74.70.Xa, 74.25.Ha, 75.60.Ch

The recently discovered iron-based superconductors [1] may exhibit new physics originating in the possible frustration of interband couplings between more than two superconducting components [2–5]. For a two-band superconductor, interband Josephson interaction either locks or antilocks phases, so that the ground state interband phase difference is respectively 0 or π. Similarly, for more than two bands, each interband coupling favors (anti)locking of the two corresponding phases. However, these Josephson terms can collectively compete so that optimal phases are neither locked nor antilocked. There, the resulting frustrated phase differences are neither 0 nor π. Since it is not invariant under complex conjugation, such a ground state spontaneously breaks the time-reversal symmetry (TRS) [2,3]. This is the $s + is$ state, with the spontaneously broken time-reversal symmetry (BTRS), that recently received strong theoretical support in connection with hole-doped $Ba_{1-x}K_xFe_2As_2$, [5]. There are also other scenarios for BTRS states in pnictides [6,7], and related multicomponent states may possibly exist in other classes of materials [8].

Symmetrywise, these BTRS states break the $U(1) \times \mathbb{Z}_2$ symmetry. The topological defects associated with the breakdown of a discrete $\mathbb{Z}_2$ symmetry are domain walls (DWs) segregating regions of different broken states [9]. Other superconductors with BTRS and having domain walls are the chiral p-wave superconductors. There are evidences for such superconductivity in Sr_2RuO_4 [10]. For that material, it is predicted that domain walls have magnetic signature and, thus, can be detected by measuring the magnetic field (see, e.g., Refs. [11,12]). These signatures were searched for in surface probes measurements, but were not experimentally detected [13]. This led to intense theoretical investigation of possible mechanisms for the field suppression (see, e.g., Ref. [14]). The problem of interaction of vortices, domain walls, and the magnetization process in these systems was studied in Refs. [15,16]. Domain walls between BTRS states are also highly important in the rotational response of ^{3}He [17]. Aspects of topological defects of the $s + is$ states received attention only recently [18–21]. The remaining question is how domain walls can be created and observed in $s + is$ superconductors. In this Letter, we demonstrate that these objects can be stabilized by geometric barriers in mesoscopic samples and discuss associated experimental signatures.

It is well known that going through a phase transition allows uncorrelated regions to fall into different ground states [22,23]. This is the Kibble-Zurek (KZ) mechanism for the formation of topological defects (see Ref. [24] for a review and Ref. [25] for a discussion in the context of chiral p-wave superconductors). As different regions fall into either of the $\mathbb{Z}_2$ states, domain walls are created while a superconductor goes through the transition to the broken

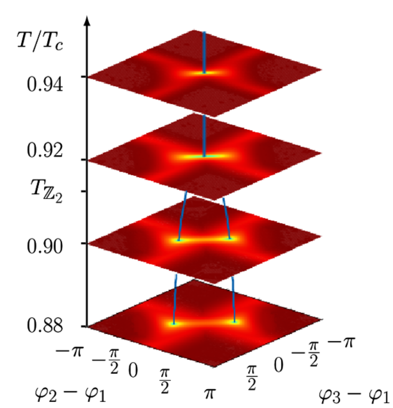

FIG. 1 (color online). This figure shows the symmetry breaking pattern for a frustrated three-band superconductor. Surfaces show the potential energy as a function of the phase differences, at different temperatures. The blue line shows the ground state. Above $T_{\mathbb{Z}_2}$, phases are locked and the ground state is unique up to overall U(1) transformations. Below $T_{\mathbb{Z}_2}$ the ground state is degenerate and time-reversal symmetry is broken.

$U(1) \times \mathbb{Z}_2$ state. Figure 1 shows the time-reversal symmetry breaking process while cooling down to the $s + is$ state (see Ref. [5] for microscopic calculations of the appearance of the $s + is$ state). Since their energy increases linearly with their length, closed domain walls contract and collapse or are absorbed by boundaries. Here we propose a mechanism to stabilize domain walls, using geometrical barriers. We use numerical simulations that mimic the KZ mechanism to depict experimental setups to nucleate, stabilize, and observe domain walls in the $s + is$ state.

We use here the minimal Ginzburg-Landau (GL) free energy functional modeling a frustrated three-band superconductor

$$\mathcal{F} = \frac{\boldsymbol{B}^2}{2} + \sum_{a=1}^{3} \frac{1}{2} |(\nabla + ie\boldsymbol{A})\psi_a|^2 + \alpha_a |\psi_a|^2 + \frac{1}{2}\beta_a |\psi_a|^4 - \sum_{a=1}^{3}\sum_{b>a}^{3} \eta_{ab} |\psi_a||\psi_b| \cos(\varphi_b - \varphi_a). \tag{1}$$

The complex fields $\psi_a = |\psi_a| e^{i\varphi_a}$ represent the superconducting condensates. They are electromagnetically coupled by the vector potential $\boldsymbol{A}$. The coupling constant e is used to parametrize the London penetration length of the magnetic field $\boldsymbol{B} = \nabla \times \boldsymbol{A}$. The temperature dependence of the coefficients is modeled as $\alpha_a \simeq \alpha_a^{(0)}(T/T_a - 1)$ [$\alpha_a^{(0)}$ and T_a being characteristic constants]. We investigate only a limited range of the reduced temperature $T/T_c \in [0.8; 1]$. In general the GL coefficients have more complicated temperature dependencies (see, e.g., Ref. [26]). However these dependencies are not very important for the questions studied here. Our results should also apply qualitatively beyond the GL regime. This is because, as shown in Ref. [5], the GL model captures the overall structure of normal modes and length scales of the full microscopic theory of the $s + is$ state.

In the frustrated regime, when all three Josephson terms cannot simultaneously attain their optimal values, the resulting ground state phase differences $\varphi_{ab} \equiv \varphi_b - \varphi_a$ are neither 0 nor π [3,4]. The ground state, thus, spontaneously breaks the time-reversal symmetry. For general consideration of phase locking between an arbitrary number of components, see Ref. [27].

As mentioned above, we model formation of domain walls during a cooling though the $\mathbb{Z}_2$ phase transition. We explore different temperature dependent routes to the TRS breaking, predicted by microscopic theory [3,5]. The first route, which we refer to as set I (see the Supplemental Material [28] for details and the chosen values of GL parameters), is the transition from the s_{++} state to the $s + is$ state. There, the system goes from a three-band TRS state to a three-band BTRS. The alternative possibility, which we refer as set II, is the transition from the $s_{\pm}$ state to the $s + is$ state, that is, from a two-band (TRS) state to three-band BTRS [3,5]. Since there are two discrete ground states, different regions of a superconductor with BTRS can fall in either the $\mathbb{Z}_2$ states and these regions are separated by domain walls created during the BTRS phase transition (at $T = T_{\mathbb{Z}_2}$). We consider field configurations varying in the xy plane, with a normal magnetic field, and assume translational invariance along the z direction. The Gibbs free energy $\mathcal{G} = \mathcal{F} - \boldsymbol{B} \cdot \mathbf{H}$ describes superconductors subject to an external field $\boldsymbol{H} = H\boldsymbol{e}_z$. To evaluate the different responses the Gibbs free energy is minimized [29] within a finite element framework provided by the FREEFEM++ library [30] (for details, see the discussion in the Supplemental Material [28]).

While a frustrated superconductor is quenched through $T_{\mathbb{Z}_2}$, the temperature of the BTRS phase transition, domain walls are created. Because of their line tension, domain walls are dynamically unstable to be absorbed by the boundaries, or collapse if they are closed. Here we propose a mechanism for stabilization of domain walls, by using a geometric barrier. Such a barrier exists in samples with nonconvex geometry, as, for example, shown in Fig. 2. Next we will show that when a domain wall is stabilized it has experimentally detectable features that can signal the $s + is$ state. As shown in Fig. 2, if during a quench a domain wall ending on nonconvex bumps is created, it can relax to a stable configuration. Indeed, to join its ends and collapse to zero size, the domain wall would have to increase its length first; it is, thus, in a stable equilibrium while trapped on the bumps. Exactly the same effect is

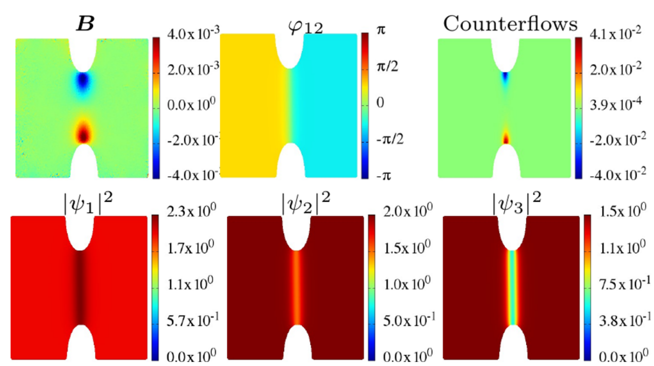

FIG. 2 (color online). A geometrically stabilized domain wall in a nonconvex domain, at $T/T_c = 0.8$ for the parameter set I. The domain wall is geometrically trapped, since to escape it should increase its length, which is energetically costly. The phase difference φ_{12} shows that during the cooling, domain walls were created and one has been stabilized by the sample's geometry. The unfavorable phase differences at the domain wall affect the densities of the condensates. $|\psi_1|^2$ overshoots at the domain wall, while $|\psi_2|^2$ and $|\psi_3|^2$ are depleted. Note that the domain wall has a magnetic signature: spots of the dipolelike magnetic field, where the domain wall touches the bumps. It originates in features of the interband counterflow at the domain wall, discussed in the text. The upper right panel shows the contribution to the magnetic field of the second term in Eq. (2).

present when there is a pinning by inhomogeneities instead of a geometric barrier (see Fig. 3). This kind of pinning induces similar magnetic dipole signatures.

To simulate cooling experiments, the energy is minimized at $T = T_c + \delta T$, i.e., starting in the normal state. The temperature is subsequently decreased with a step δT and the energy minimized for the new temperature (i.e., new α_a's). The faster the system undergoes a phase transition, the more defects are nucleated. This is achieved, in our simulations, by cooling with bigger temperature steps (see the animations in the Supplemental Material [28] for a typical domain-wall–stabilizing process). Domain walls are always created, but their location is random and, thus, they do not always geometrically stabilize. We performed several simulations of the cooling processes and verified that indeed the number of produced defects is larger when temperature steps are bigger. Conversely, to ensure that no DW is formed, the system has to be cooled very slowly.

Remarkably, as shown in Figs. 2 and 3, even in zero applied field the domain wall carries opposite, nonzero magnetic field at its ends. Yet the total net flux through the sample is zero. The magnitude of this effect depends on the width of the domain wall (and, thus, on the parameters of the model). For Fig. 2, the amplitude of the local fields is of the order of magnitude of a percent of the magnetic field of a vortex. The origin of this signature in the $s + is$ state is principally different from the magnetic signature of domain walls in a $p + ip$ superconductor. Namely, in $p + ip$ superconductors, DWs carry uniform magnetic field originating from mechanisms which do not have a counterpart in $s + is$ superconductors (see, e.g., Refs. [12,14,25]). Here, by contrast, the domain walls carry magnetic field only where they are attached to the boundary and the field inverts its direction so that there is no net flux. This magnetic field originates in interband counterflow in the presence of relative density gradients. Indeed, the magnetic field has the following dependence on the field gradients [20]:

$$B_z = -\epsilon_{ij}\partial_i\left(\frac{J_j}{e|\Psi|^2}\right) - \frac{i\epsilon_{ij}}{e^2|\Psi|^4}[|\Psi|^2\partial_i\Psi^\dagger\partial_j\Psi + \Psi^\dagger\partial_i\Psi\partial_j\Psi^\dagger\Psi], \tag{2}$$

with $\Psi^\dagger = (\psi_1^*, \psi_2^*, \psi_3^*)$ and $|\Psi|^2 = \Psi^\dagger\Psi$. The interband counterflow contribution to $\boldsymbol{B}$ is the second term in Eq. (2), that is, density gradients mixed with gradients of phase differences (see Figs. 2 and 3). In the total magnetic field signature, counterflows are partially screened by the first term in Eq. (2).

For modeling field cooled experiments, the Gibbs energy for a given applied field H is minimized for decreasing temperatures. This is shown in Fig. 4. At T_c superconductivity sets in and the sample is filled with vortices. Then while the temperature is further decreased, past the $\mathbb{Z}_2$ phase transition (at $T_{\mathbb{Z}_2}$), the KZ mechanism leads to the formation of domain walls. As shown in Fig. 4, the preexisting vortices stabilize the domain walls against collapse (regardless of the geometry). These domain walls are either closed or terminate on the boundary. Closed domain walls stabilized by vortices were considered in Refs. [18,20]. Being characterized by $\mathbb{C}P^2$ topological invariant, these are Skyrmions. Note that to accommodate the unfavorable phase differences at the DW, it is beneficial to split vortices into three types of fractional vortices (see the detailed discussion in Refs. [18,20]). At the DW, the vortices are less localized and their magnetic signature is more smeared out. The DW can clearly be identified when measuring the magnetic field.

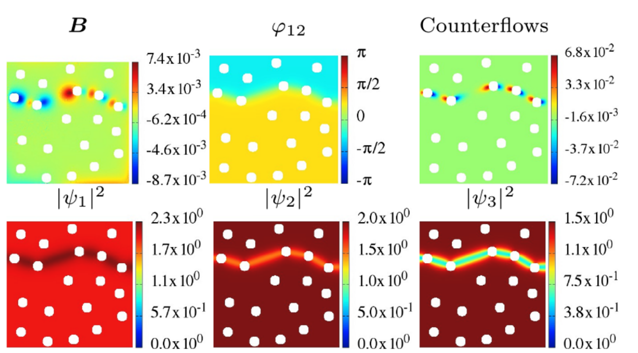

FIG. 3 (color online). A domain wall stabilized by randomly located pinning centers. When cooled past $T_{\mathbb{Z}_2}$, domain walls are formed at random positions. Then, during the relaxation process, the quench-induced domain wall is stabilized against collapse by nearby pinning centers. Displayed quantities and physical parameters are the same as in Fig. 2. Here again, the domain wall has a dipolelike signature of the magnetic field where it is attached to the pinning centers.

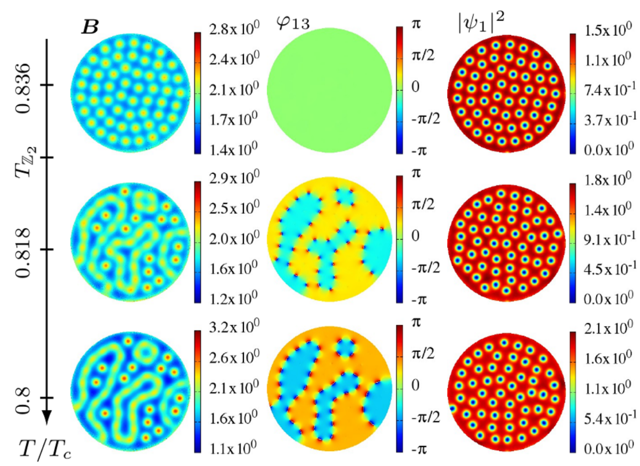

FIG. 4 (color online). Field cooled experiment for the parameter set II, under an applied field $H/\Phi_0 S = 70$. First, the system is a two band ($\psi_2 = 0$) and, thus, it is TRS. When cooled through $T_{\mathbb{Z}_2}$ ($\psi_2 \neq 0$) the system enters the BTRS regime and different regions pick up different ground state phase locking. The resulting DWs are stabilized against complete contraction by the already existing vortices.

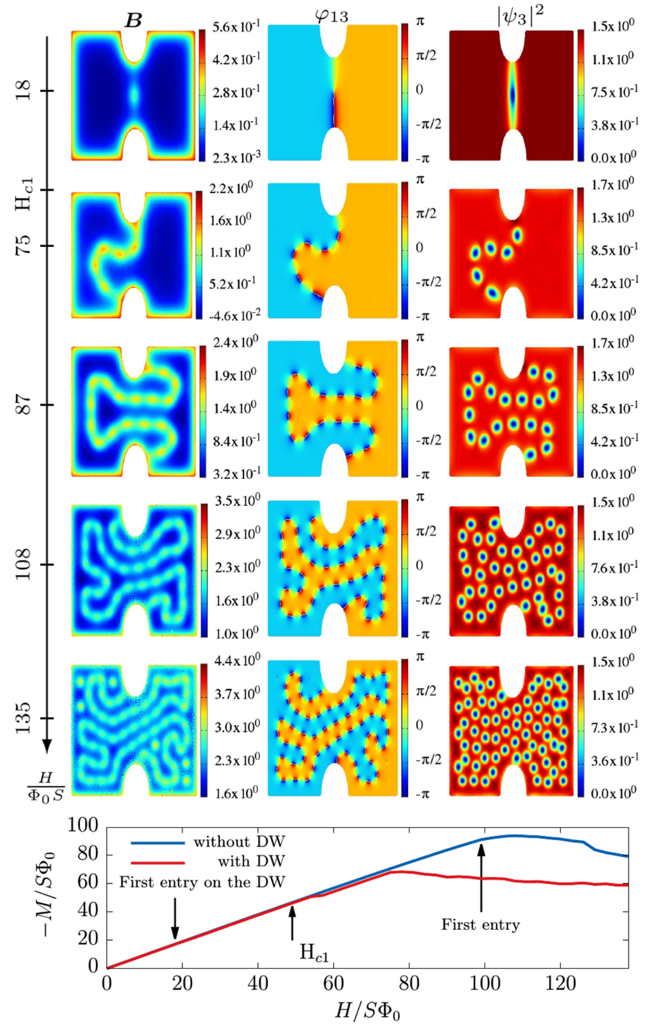

FIG. 5 (color online). Magnetization process of a three-band BTRS, when the zero field configuration has the geometrically stabilized domain wall (Fig. 2). First, vortex entry, way below H_{c1}, shown in the top row is a fractional vortex in ψ_3. This can be seen from the phase difference φ_{13} which winds 2π. The red curve is the corresponding magnetization curve, while the blue curve is a reference magnetization, starting from a uniform ground state.

Consider now the magnetization process at fixed $T < T_{\mathbb{Z}_2}$. No field is initially applied ($H = 0$) and the superconductor is in one ground state. The applied field is increased with a step δH. There are no preexisting DWs and, as long as the applied field is below H_{c1}, no vortex enters. The Meissner state survives to fields higher than H_{c1} because of the Bean-Livingston barrier. While the applied field is further increased, vortices enter and arrange in a triangular lattice. Note that big steps δH can provide enough energy to locally fall into the opposite $\mathbb{Z}_2$ state during a relaxation process. This leads to the formation of a domain wall, which is stabilized by the presence of vortices (see the Supplemental Material [28]).

Now we consider the regime of our main interest. As shown in Fig. 5, the magnetization process in the presence of a quench-induced and geometrically stabilized domain wall is very unusual. The first vortex entry occurs at much lower fields than H_{c1}. Here, a core is created only in one band; thus, it is a fractional vortex that enters the domain wall. Fractional vortices are thermodynamically unstable in a uniform bulk superconducting state because they have logarithmically divergent energy [20]. The situation here is different because the sample has a preexisting domain wall. See the Supplemental Material [28] for all quantities. In increased field the domain wall is filled with vortices. Despite its energy cost, it eventually becomes beneficial to elongate the domain wall. It starts bending and gradually fills the sample. At the first integer vortex entry, the sample is already filled by the flux-carrying DW. The associated magnetization curve also shows striking differences from the case without domain walls. This can provide a way to confirm $s + is$ superconductivity. For a sample whose geometry allows stabilization of DWs, the magnetization process after a rapid cooling (or other kind of quench) can be significantly different from that of the same, slowly cooled sample. The first will show a magnetization process different from the reference measurement. Chances to stabilize the domain walls are further enhanced by having multiple stabilizing geometric barriers.

In conclusion, we have studied domain walls in $s + is$ superconductors. We presented a proposal for an experimental setup that can lead to formation of stable domain walls. We demonstrated that domain walls in $s + is$ superconductors have magnetic signatures that could be detected in scanning SQUID, Hall, or magnetic force microscopy measurements. Moreover we showed that for a geometrically stabilized DW, the magnetization curve could change substantially as the DW allows flux penetration in the form of fractional vortices in low fields. Thus, a sample subject to different cooling processes should exhibit very different magnetization processes and magnetization curves.

The observation of these features can signal the $s + is$ state (because, in contrast, the $s_{\pm}$ and s_{++} states do not break $\mathbb{Z}_2$ symmetry and, thus, have no domain walls), for example, in hole-doped $Ba_{1-x}K_xFe_2As_2$ [5].

We acknowledge fruitful discussions with J. Carlström and D. Weston. This work is supported by the Swedish Research Council, by the Knut and Alice Wallenberg Foundation through a Royal Swedish Academy of Sciences fellowship and by NSF CAREER Grant No. DMR-0955902. The computations were performed on resources provided by the Swedish National Infrastructure for Computing (SNIC) at the National Supercomputer Center at Linkoping, Sweden.

*garaud.phys@gmail.com

[1] Y. Kamihara, T. Watanabe, M. Hirano, and H. Hosono, J. Am. Chem. Soc. **130**, 3296 (2008).
[2] T. K. Ng and N. Nagaosa, Europhys. Lett. **87**, 17003 (2009).
[3] V. Stanev and Z. Tesanovic, Phys. Rev. B **81**, 134522 (2010).
[4] J. Carlström, J. Garaud, and E. Babaev, Phys. Rev. B **84**, 134518 (2011).
[5] S. Maiti and A. V. Chubukov, Phys. Rev. B **87**, 144511 (2013).
[6] W.-C. Lee, S.-C. Zhang, and C. Wu, Phys. Rev. Lett. **102**, 217002 (2009).
[7] C. Platt, R. Thomale, C. Honerkamp, S.-C. Zhang, and W. Hanke, Phys. Rev. B **85**, 180502 (2012).
[8] S. Mukherjee and D. F. Agterberg, Phys. Rev. B **84**, 134520 (2011).
[9] N. S. Manton and P. Sutcliffe, *Topological Solitons* (Cambridge University Press, Cambridge, England, 2004).
[10] J. Xia, Y. Maeno, P. T. Beyersdorf, M. M. Fejer, and A. Kapitulnik, Phys. Rev. Lett. **97**, 167002 (2006).
[11] M. Matsumoto and M. Sigrist, J. Phys. Soc. Jpn. **68**, 994 (1999).
[12] D. G. Ferguson and P. M. Goldbart, Phys. Rev. B **84**, 014523 (2011).
[13] C. W. Hicks, J. R. Kirtley, T. M. Lippman, N. C. Koshnick, M. E. Huber, Y. Maeno, W. M. Yuhasz, M. B. Maple, and K. A. Moler, Phys. Rev. B **81**, 214501 (2010).
[14] S. Raghu, A. Kapitulnik, and S. A. Kivelson, Phys. Rev. Lett. **105**, 136401 (2010).
[15] Y. Matsunaga, M. Ichioka, and K. Machida, Phys. Rev. B **70**, 100502 (2004).
[16] M. Ichioka, Y. Matsunaga, and K. Machida, Phys. Rev. B **71**, 172510 (2005).
[17] P. M. Walmsley and A. I. Golov, Phys. Rev. Lett. **109**, 215301 (2012).
[18] J. Garaud, J. Carlström, and E. Babaev, Phys. Rev. Lett. **107**, 197001 (2011).
[19] S.-Z. Lin and X. Hu, New J. Phys. **14**, 063021 (2012). This work studied dynamics of unstable closed domain walls and reported appearance of magnetic signatures. We did not observe this kind of magnetic signatures in our simulations, which by contrast focuses on (quasi-)equilibrium configurations.
[20] J. Garaud, J. Carlström, E. Babaev, and M. Speight, Phys. Rev. B **87**, 014507 (2013).
[21] T. Bojesen, E. Babaev, and A. Sudbø, arXiv:1306.2313.
[22] T. W. B. Kibble, J. Phys. A **9**, 1387 (1976).
[23] W. H. Zurek, Nature (London) **317**, 505 (1985).
[24] R. Rivers, J. Low Temp. Phys. **124**, 41 (2001).
[25] V. Vadimov and M. Silaev, Phys. Rev. Lett. **111**, 177001 (2013).
[26] M. Silaev and E. Babaev, Phys. Rev. B **85**, 134514 (2012).
[27] D. Weston and E. Babaev, Phys. Rev. B **88**, 214507 (2013).
[28] See Supplemental Material at http://link.aps.org/supplemental/10.1103/PhysRevLett.112.017003 for details of the parameters and numerical methods. Animations of the magnetization processes and field cooled experiments are also available.
[29] Note that the KZ mechanism involves actual time dependence. In our approach, we use a minimization algorithm instead of solving the actual time-dependent equations. At each temperature, once the algorithm has converged, the system is stationary. Then the temperature is changed by a certain amount δT and minimization is repeated. Thus, we do not simulate the actual Kibble-Zurek dynamical problem. Rather, it is a quasiequilibrium process that mimics the features of the KZ mechanism. Our quasiequilibrium simulation accounts for a number of features that would happen in the actual time-dependent evolution (such as spontaneous domain wall formation when the step δT is sufficiently large, which corresponds to a rapid cooling). While we cannot predict the rate for formation of topological defects, this simulation is sufficient to study the problem of geometric stabilization.
[30] F. Hecht, O. Pironneau, A. Le Hyaric, and K. Ohtsuka, The Freefem++ Manual (Universite Pierre et Marie Curie, Paris, 2007), 3rd ed.